Recent advances in light-emitting electrochemical cells*

Rubén D. Costa[1,2,‡], Enrique Ortí[1], and Henk J. Bolink[1]

[1]*Instituto de Ciencia Molecular, Universidad de Valencia, 46980 Paterna (Valencia), Spain;* [2]*Current address: Department of Chemistry and Pharmacy and Interdisciplinary Center for Molecular Materials (ICMM), Friedrich-Alexander-Universität Erlangen-Nürnberg, Egerlandstrasse 3, 91058 Erlangen, Germany*

Abstract: Light-emitting electrochemical cells (LECs) are solution-processable thin-film electroluminescent devices consisting of a luminescent material in an ionic environment. The simplest type of LEC is based on only one material, ionic transition-metal complexes (iTMCs). These materials are of interest for different scientific fields such as chemistry, physics, and technology as selected chemical modifications of iTMCs resulted in crucial breakthroughs for the performance of LECs. This short review highlights the different strategies used to design these compounds with the aim to enhance the performances of LECs.

Keywords: ionic transition-metal complexes; iridium complexes; light-emitting electrochemical cells; lighting devices.

INTRODUCTION

Light-emitting electrochemical cells (LECs) are a promising new type of lighting device. They are single-layer electroluminescent devices consisting of a luminescent material in an ionic environment [1,2]. The luminescent material is either a conjugated light-emitting polymer in combination with inorganic salts or an ionic transition-metal complex (iTMC) used in polymer-based LECs (PLECs) or iTMC-LECs (Fig. 1). The main characteristic of these devices is their insensitivity to the work function of the electrodes employed, owing to the role of the mobile ions in the operation mechanism. Currently, there are three models competing to be accepted, namely: (a) electrochemical [1,3–8], (b) electrodynamic [9–13], and (c) a unified model [14,15]. Nevertheless, all models agree that the key of the mechanism in LECs is the assistance of the mobile anions to the injection process. Therefore, in contrast to conventional organic light-emitting diodes (OLEDs), air-stable electrodes, such as gold, silver, or aluminum, can be used, and as a consequence their encapsulation does not have to be as rigorous as with OLEDs.

iTMC-LECs are based on only one active component, and thus they can be considered to be the simplest kind of electroluminescent device (Fig. 1b). iTMCs can support all three necessary processes for electroluminescence, namely: charge injection, charge transport, and emissive recombination. Although high power efficiency, short turn-on time, and reasonable lifetimes have been achieved individually in green and orange LECs, there is no single device having all those properties, and there are also few reports of blue-emitting devices. Accordingly, there is much scope for continuing research to progress in this field of simple light-emitting devices.
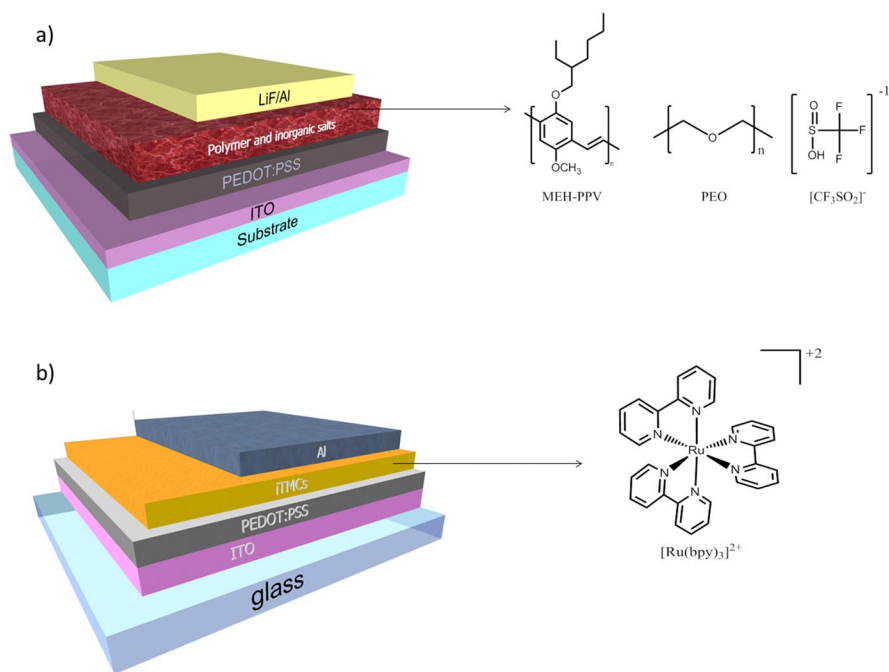
Fig. 1 Schematic representation of a typical PLEC (a) and iTMC-LEC (b). Top: Typical materials used in PLECs. MEH-PPV is the poly[5-(2'-ethylhexyloxy)-2-methoxy-1,4-phenylene vinylene], PEO is poly-(ethylene oxide), and $[CF_3SO_3]^-$ is trifluoromethyl sulfonate. Bottom: Typical materials used in iTMC-LECs. $[Ru(bpy)_3]^{2+}$ where bpy is 2,2'-bypiridine.

The initial experiments performed on iTMC-based LECs were carried out using the $[Ru(bpy)_3]^{2+}$ cation balanced by different counter-anions (Fig. 1b) [16–21]. Other iTMCs, such as ionic osmium(II) or copper(I) complexes, have also been used to fabricate LECs (Fig. 2) [22–29]. However, the best performance levels in LECs have been observed using heteroleptic iridium(III) complexes, hereafter abbreviated as Ir-iTMCs (Fig. 2b) [2,30]. In its simplest form, the Ir-iTMCs used in LECs consist of a combination of at least two different ligands, one ancillary ligand (N^N), such as ethylendiamine (en), 2,2'-bipyridine (bpy), 1,10-phenantroline (phen), 2-(1H-pyrazol-1-yl)pyridine (pzpy), 2-(1-phenyl-1H-imidazol-2-yl)pyridine (pyim), etc., and two cyclometalating ligands (C^N), such as 2-phenylpyridine (Hppy), 1-phenylpyrazol (Hppz), etc. Their abbreviated structure is $[Ir(C^N)_2(N^N)]^{+1}$.
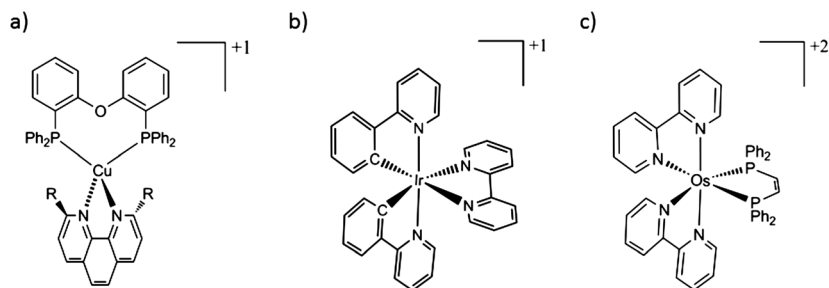
Fig. 2 Chemical structure of several iTMCs conventionally used as the unique electroactive material in LECs. For more information, see refs. [29] (a), [31] (b), and [22] (c).

All the improvements recently reached in iTMC-LECs have been achieved using different Ir-iTMCs [14,30–67]. There are several reasons that justify the selection of Ir-iTMCs over other complexes like Ru-iTMCs. First, the dissociative metal-centered (^{3}MC) excited states are less accessible, which leads to an enhancement of the photostability compared to Ru-iTMCs [68–72]. Second, the high photoluminescence quantum yields (PLQY or ϕ) observed for Ir-iTMCs compared to those reported for Ru-iTMCs are due to the larger spin-orbit coupling resulting from the third-row Ir(III) ion [69,73]. Third, the frontier molecular orbitals in these Ir-iTMCs are well located over different regions of the complex. The highest occupied molecular orbital (HOMO) is usually composed of the π-HOMO of the C^N ligands and the dπ orbital of the metal, whereas the lowest unoccupied molecular orbital (LUMO) is located on the ancillary ligand (Fig. 3). The nature of the emitting excited triplet state, which is normally described as a monoelectronic transition HOMO → LUMO, presents a mixed character of metal-to-ligand and ligand-to-ligand charged transfer (MLCT and LLCT, respectively). Therefore, depending on independent chemical modifications of both ligands, the HOMO–LUMO energy gap in these complexes can be easily tuned. This has led to the development of ionic emitters in the entire visible spectrum region [33,35,42,47,53,63,64,74–76].
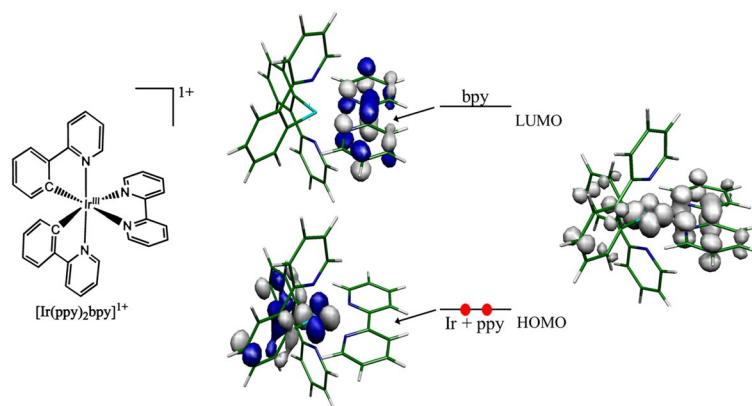
Fig. 3 Schematic diagram showing the electronic density contours (0.05 e bohr^{-3}) calculated for the frontier molecular orbitals (middle) and the spin density calculated (right) for the optimized triplet emitting states of the [Ir(ppy)$_2$(bpy)]$^{+1}$.

Taking into account the above-discussed properties of Ir-iTMCs, the C^N (Hppy and Hppz) and N^N (bpy and phen) ligands showing different substitution schemes are selected and combined to build up complexes with desired properties for obtaining better performances in LECs. In this brief review we present a selection of specific Ir-iTMCs that have provided important breakthroughs in LECs concerning different points such as color, efficiency, and stability, which were achieved in the framework of the first author's thesis. This work is presented in several sections concerning the color emission (deep-red, orange, green, and blue regions) together with the most important achievements reported for LECs to date.

## ELECTROFLUORESCENCE OF DEEP-RED LECs

Only a few examples of LECs have been reported that emit in the deep-red or infrared regions using single iTMCs as the main component [35,56,77,78]. The main reason for this is the lack of iTMCs with low HOMO–LUMO energy gaps that show phosphorescence emission with high PLQYs. Red emitters have been usually designed by attaching electron-withdrawing groups on the N^N ligand or by using

N^N ligands with a low-energy LUMO such as the biq ligand (2,2'-biquinoline) [35,53,56,74,76]. A new plausible alternative that involves the chemical attachment of a fluorescent emitter that has a high PLQY to an iTMC has been recently presented [51,79]. Perylenediimides (PDIs) were selected as a fluorescent emitter because of their exceptional photochemical stability, their high fluorescence quantum yields in the deep-red region, and their good electron-transport properties [80]. We demonstrated that the synergistic collaboration between an Ir-iTMC (that functions as the hole conductor) and a red fluorescent PDI emitter (that is an electron-transporting material and shows high PLQY), leads to highly efficient emission in the deep-red region.

In this new compound $[Ir(ppy)_2(phen-PDI)][PF_6]$ (Fig. 4a), the PDI moiety is directly attached to the Ir-iTMCs to avoid phase separation processes due to their different natures. The optimized molecular structure of this complex shows that both moieties are in a perpendicular configuration, which indicates that they are electronically decoupled. The HOMO and LUMO are located on the PDI part and correspond to the π HOMO and LUMO of PDI, respectively (Fig. 4b). Therefore, the topology of the frontier orbitals suggests that emission should originate from the PDI fragment. Indeed, the photoluminescence spectrum exhibits a structured band at 619 nm, similar to the fluorescence spectra of previously reported PDI compounds [81], and different from the phosphorescence spectrum of the iridium complex (Fig. 4c). In addition, the high PLQY (55 %, by irradiation of the PDI unit) and the low excited-state lifetime (3.0 ns) recorded for the emission unambiguously indicate that the emitting state is the lowest excited singlet state of the PDI part of the molecule.

This compound was tested in LECs [51]. The features of the electroluminescence spectrum recorded at 3 V (Fig. 4c) are similar to those observed for the photoluminescence registered in solution, which indicates that the electroluminescence process occurs from the excited singlet state located on the PDI. The CIE coordinates of the emitted light are $x = 0.654$ and $y = 0.344$ and correspond to a deep-red color [82].

Upon applying a bias of 3 V to the device (Fig. 4d), the luminance reaches values slightly higher than those reported for iTMC-based LECs that emit in the same wavelength region [56,77,78]. In fact, high values of current efficiency (2.5 cd/A), maximum power efficiency (2.56 Lm/W), and external quantum efficiency (3.27 %) are reached after approximately 22 min of device operation. These values are the highest reported for LECs in the deep-red or near-infrared region. This improvement is attributed to the combination of two effects: (a) the high PLQY (55 %), which increases the radiative recombination, and (b) the low lifetime of the generated excitons (3 ns), which decreases its diffusion time. Thus, nonradiative decay processes via impurities or grain defects [83] have a lower probability to occur.
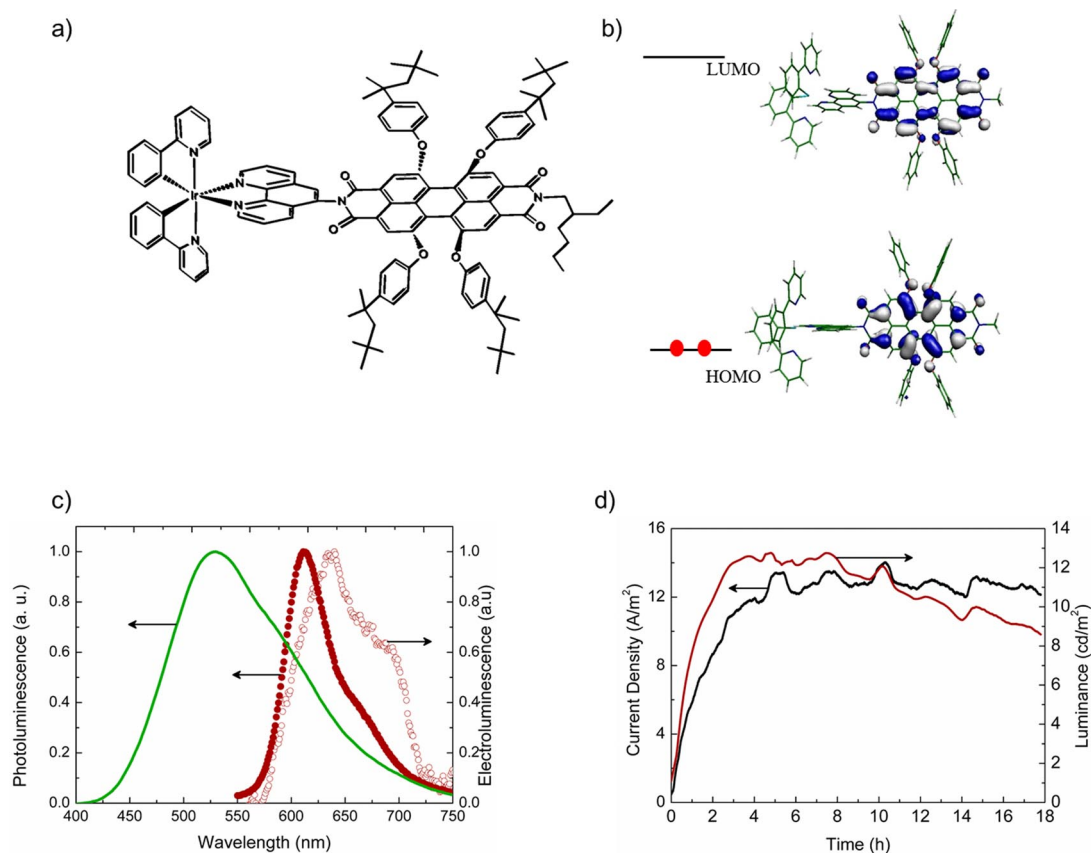
Fig. 4 (a) Chemical structure of the compound [Ir(ppy)$_2$(phen-PDI)][PF$_6$]. (b) Electronic density contours (0.05 e bohr^{-3}) calculated for the HOMO and LUMO of this complex. (c) Photoluminescence spectra of the complex [Ir(ppy)$_2$(phen)][PF$_6$] (green line) and compound [Ir(ppy)$_2$(phen-PDI)][PF$_6$] (full red circles) in acetonitrile solution. Electroluminescence spectrum of the LEC device based on compound [Ir(ppy)$_2$(phen-PDI)][PF$_6$] (open red circles) at an applied bias of 3 V. (d) Current density and luminance vs. time at an applied voltage of 3 V for an LEC device based on [Ir(ppy)$_2$(phen-PDI)][PF$_6$].

STABLE ORANGE LECs

The stability of LECs is defined as either the lifetime [$t_{1/2}$ (h), time to reach half of the maximum luminance value] or the total emitted energy [E_{tot} (J), a value that results from the integration of the radiant flux vs. time from $t = 0$ (application of bias) to $t = t_{1/5}$] [84].

It is well established that the stability of LECs based on [Ru(bpy)$_3$][PF$_6$]$_2$ is determined by the degradation of this complex during the device operation [84–86]. Two works evidenced the formation of the oxo-bridged dimer [Ru(bpy)$_2$(H$_2$O)]$_2$O[PF$_6$]$_4$ as quencher in [Ru(bpy)$_3$][PF$_6$]$_2$ devices [85,86]. The dimer probably results from the condensation of two molecules of the [Ru(bpy)$_2$(H$_2$O)$_2$]$^{2+}$ quencher previously proposed [84]. The degradation mechanism of the iTMCs is described as an exchange reaction in which the ancillary ligand (bpy) is replaced by two nucleophilic molecules (H$_2$O) when the metal-centered excited states (^{3}MC) are populated [68,69,71,72]. The nucleophilic molecules make their closest approach to the metal core through the octahedral faces of the open coordination sphere. Hence, the protection of the coordination sphere of the complex against the entrance of nucleophilic molecules is highly desirable to design stable iTMCs.

Following this idea, several works have recently been reported in which designed supramolecularly caged Ir-iTMCs lead to long-living LECs [31,45,46,52,59,60,65,67]. The supramolecularly caged conformation is obtained by using intramolecular π–π interaction, which is obtained by attaching a phenyl group to the ancillary ligand (Fig. 5).
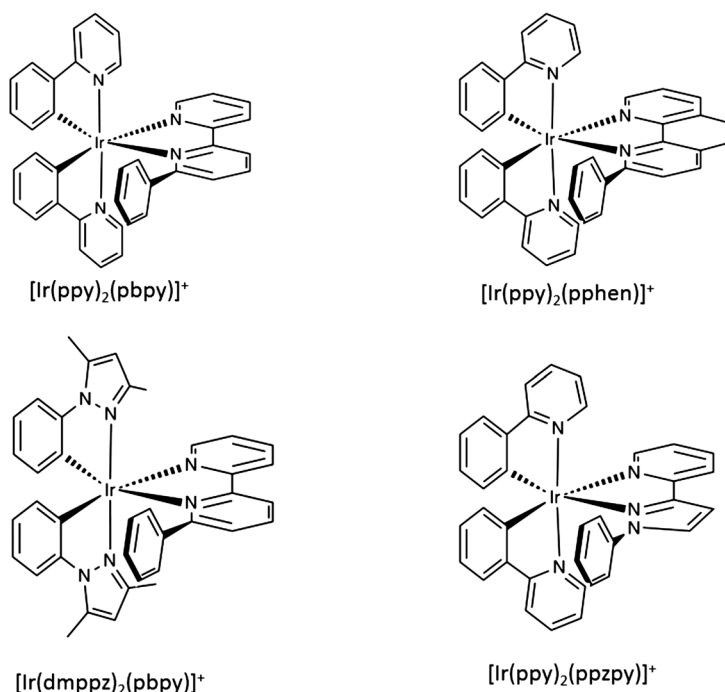
Fig. 5 Chemical structure of complex $[Ir(ppy)_2(pbpy)][PF_6]$ where pbpy is 6-phenyl-2,2'-bipyridine [45], complex $[Ir(dmppz)_2(pbpy)][PF_6]$ where dmppz is 3,5-dimethyl-1-phenylpyrazole [60], complex $[Ir(ppy)_2(pphen)][PF_6]$ where pphen is 2-phenyl-1,10-phenanthroline [65], and complex $[Ir(ppy)_2(ppzpy)][PF_6]$ where ppzpy is 2-(1-phenyl-1*H*-pyrazol-3-yl)pyridine [67].

One of the latest breakthroughs in the stability of LECs was obtained using the complex $[Ir(dmppz)_2(pbpy)][PF_6]$ (Fig. 5) [60]. Figure 6 depicts the X-ray structure of the cation in the lattice of $[Ir(dmppz)_2(pbpy)][PF_6]$. It shows the same intracation face-to-face π-stacking of the pendant phenyl ring of the pbpy ligand as observed in similar complexes [45,46,52,59,60]. The π-stacking interaction is observed between the rings containing C1 and C33 (centroid–centroid distance, 3.51 Å). Density functional theory (DFT) calculations on the ground state of this complex show that the topologies of the HOMO and LUMO are similar to those described for similar Ir-iTMCs (Fig. 6) [31,35,59].

The photophysical properties of this complex are characterized by an unstructured and broad photoluminescence spectrum with a maximum emission wavelength of 574 nm. The PLQY and the excited-state lifetime in de-aerated acetonitrile solution (λ_{exc} = 355 nm) were 2 % and 0.6 μs, respectively. As expected, the nature of the emitting triplet state (T_1) is a mixed $^3MLCT/^3LLCT$ character resulting from the HOMO → LUMO excitation (Fig. 6c). DFT calculations show that the π-stacking interaction is preserved in the T_1 and ^3MC excited triplet states with centroid–centroid distances of 3.58 and 3.78 Å, respectively. The intramolecular π–interaction determines that in the ^3MC state the $Ir–N_{dmppz}$ bond implying the dmppz ligand where the π-stacking is present is significantly shorter (0.20 Å) than the other $Ir–N_{dmppz}$ bond. This fact has been also observed in other supramoleculary
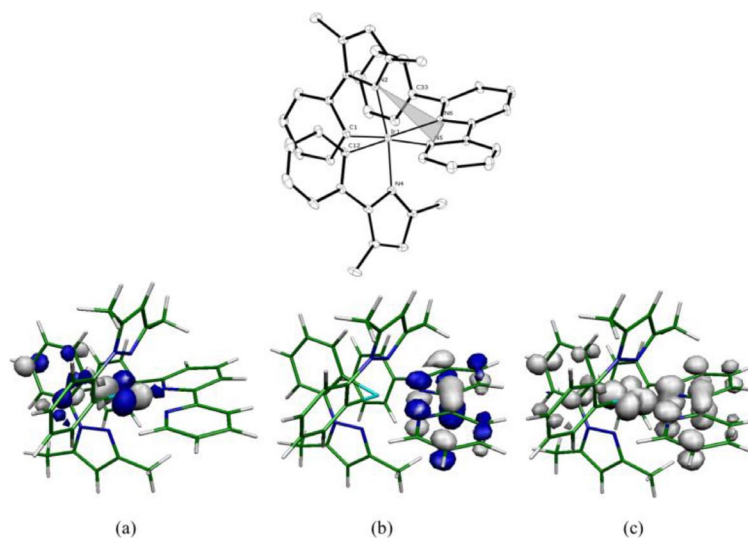
Fig. 6 Top: X-ray structure of the [Ir(dmppz)$_2$(pbpy)]$^+$ cation showing the intracation face-to-face π-stacking of the pendant phenyl ring containing C33 with the cyclometalated phenyl ring containing C1 of a dmppz ligand. Hydrogen atoms have been omitted for clarity, and thermal ellipsoids are represented at 50 % probability. Bottom: Electronic density contours (0.05 e bohr^{-3}) calculated for the HOMO (a) and the LUMO (b) of [Ir(dmppz)$_2$(pbpy)]$^+$ cation in its S$_0$ ground state. (c) Spin density distribution (0.005 e bohr^{-3}) calculated for [Ir(dmppz)$_2$(pbpy)]$^+$ cation in the T$_1$ excited state.

caged complexes [45,46,52,59,60]. Hence, this π–π interaction leads to the formation of a stable supramolecular cage conformation both in the ground and in the excited states (emitting and ^{3}MC states) of the Ir-iTMCs, which should reduce the degradation process and lead to highly stable LECs.

LECs employing the above-mentioned complex were prepared showing high lifetime both expressed as $t_{1/2}$ (2000 h) and E_{tot} (18.7 J). These values were significantly the highest values reported up to now using a constant applied voltage of 3 V. Furthermore, these LECs also show a high stability at high applied voltages, which confirms their robustness against the degradation process.

The main reason for this behavior is the combination of two synergic effects: the intramolecular π–π interaction and the presence of methyl groups that help in blocking the entrance of nucleophilic molecules (Fig. 6, top). The pendant methyl groups of the dmppz ligands are located over the octahedral faces containing the N^N ligand and are a clear impediment to the entrance of nucleophilic molecules, thus rendering the degradation more difficult. Therefore, the use of alkyl groups in these positions additionally protects the iTMC against degradation, thus explaining the improvement in the stability of LECs. This assumption is also corroborated by the lower stabilities ($t_{1/2}$ 142 h and E_{tot} 0.33 J) of LECs employing a similar complex without the methyl groups on the pyrazole ligands.

Recently, another group has adopted this strategy, and this group also obtains a significant enhancement of the stability [67].

EFFICIENT GREEN LECs

The efficiency of iTMC-based LECs depends primarily on the PLQY of the complex in film [44]. The PLQY for most of the Ir-iTMCs is low in a film with the same composition as in the active layer used in LECs. The reason is the strong self-quenching produced by the proximity of the complexes. Slinker et al. reported one of the most promising strategies to increase the PLQY of Ir-iTMCs, which led to highly efficient LECs [30]. This strategy consists of the attachment of bulky groups to the periphery of

the ligands. The bulky groups separate the complexes in the solid state and lead to high PLQY values in a film [30,43,57,59,87]. In particular, Slinker et al. showed that the [Ir(ppy)$_2$(dtb-bpy)][PF$_6$] complex (dtb is 4,4'-di-*tert*-butylbipyridine) gives rise to efficient LECs (10 Lm/W) [30]. The use of the fluorinated version of the later complex [Ir(F$_2$-ppy)$_2$(dtb-bpy)][PF$_6$] [F$_2$-ppy is 2-(2',4'-difluorophenyl)pyridine] also led to highly efficient green LECs (39.8 Lm/W at 3 V and 21 Lm/W at 4 V) [44]. The photoluminescence recorded in acetonitrile solution and the electroluminescence spectra shows the same profile emission with a maximum at ~512 nm. The emission is considerably shifted compared to that of the [Ir(ppy)$_2$(bpy)][PF$_6$] complex (585 nm) [31] owing to the effect of the attached groups (electron-withdrawing fluorine atoms and electron-donating *tert*-butyl groups on the ppy and bpy ligands, respectively) on the energy position of the HOMO and LUMO. DFT calculations clearly indicate that the use of F$_2$-ppy and dtb-bpy ligands results in a significant stabilization of the HOMO and destabilization of the LUMO compared to those of [Ir(ppy)$_2$(bpy)]$^{1+}$ [31,44]. Su et al. demonstrated that the bulky groups in [Ir(F$_2$-ppy)$_2$(sb)][PF$_6$] complexes (sb is 4,5-diaza-9,9'-spirobifluorene) inhibit nonradiative pathways associated with the self-quenching [43]. This was reflected in the power efficiencies, which had a value of 26.1 Lm/W in the green region (535 nm). Bryce and Monkman et al. [57] reported a series of [Ir(ppy)$_2$(N^N)][PF$_6$] complexes, on which several bulky 9,9-dihexylfluorene and 9,9-carbazolyl-fluorene side groups were attached to the bpy and phen ligands. They demonstrated that the addition of bulky groups has little effect on the electronic properties of the complex and only enhances the steric hindrance that reduces the self-quenching in thin films. Thus, they provide efficient LECs with current efficiencies of 7 cd/A. However, the use of even bulkier groups induces an undesired reduction of the charge carrier mobility, as a consequence of the larger intermolecular separation. Similar results were also obtained in our group studying a series of supramolecularly caged complexes in which the size of the bulky groups increases [59]. They demonstrated that the use of bulky groups provides two main effects on LECs: (a) the efficiency increases because of the reduction of the self-quenching in the thin film, and (b) the stability also enhances because of the hydrophobic character of the Ir-iTMCs.

Another plausible strategy to increase the average intersite distance between iTMCs is to connect two Ir-iTMCs by a rigid π-conjugated spacer. Novel green-emitter dumbbell-shaped dinuclear Ir-iTMCs (Fig. 7) incorporating the oligophenylene ethynylene spacer endowed with two bipyridyl units have been recently reported [58]. The terminal bipyridyl units are used to link two heteroleptic Ir-iTMCs whose coordination sphere is completed with two F$_2$-ppy ligands. The photoluminescence of the spacer is characterized by a poorly resolved structured band with maximum emission at 443 nm (Fig. 7). In contrast, the photoluminescence of the dinuclear compound is described as a broad structureless band in the green region (521 nm). The shape of the band and the emission maximum recorded for the dinuclear Ir-iTMCs perfectly agree with those obtained for the end-capping Ir-iTMCs (Fig. 7). Hence, the nature of the emitting excited state is ascribed to the phosphorescence of the end-capping iTMCs. However, this compound presents very poor photophysical properties. The dinuclear complex shows a very low PLQY of 0.7 % compared to that measured for the end-capping Ir-iTMCs (18 %). We demonstrated this result by using transient absorption experiments in the μs time domain in combination with DFT calculations that the lowest triplet state of the dinuclear compound corresponds to a ^{3}π–π state located on the conjugated spacer. The appearance of this state below the emitting states of the end-capping Ir-iTMCs effectively quenches the phosphorescent emission from the iTMCs and leads to very low photoluminescent performances.

Standard LECs based on this compound show an electroluminescent emission in the green region (CIE coordinates: *x* = 0.3696, *y* = 0.4625) [82] with a maximum at 540 nm (Fig. 7). It was shown that the self-quenching caused by high iTMC concentration in the device was reduced.
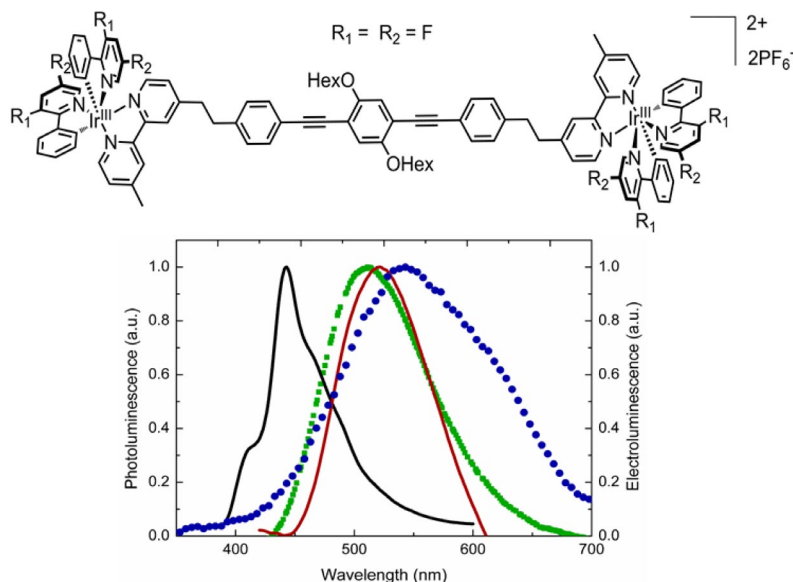
Fig. 7 Top: Chemical structure of the dinuclear Ir-iTMCs. Bottom: Photoluminescence spectra of the dinuclear compound (red line) and the end-capping Ir-iTMCs (green circles) in de-aerated acetonitrile (~10^{-6} M) and of the spacer (black line) in *o*-dichlorobenzene (~10^{-6} M). Electroluminescence spectrum (blue circles) of an LEC device based on the dinuclear compound at 3 V is also shown.

DESIGNING LIGANDS FOR BLUE LECs

As mentioned above, two general strategies have been used to shift the emission to the blue region. One way is to attach electron-withdrawing substituents onto the phenyl groups of the ppy ligand, which stabilizes the HOMO, and electron-donating substituents onto the bpy ligand, which destabilizes the LUMO [35,74,76]. Thus, the HOMO–LUMO energy gap is enlarged and the emission color shifts toward the green/blue region. The second strategy is to use different types of C^N and N^N ligands. For instance, Tamayo et al. used a F_2-ppz ligand [C^N ligand, F_2-ppz is 1-(4,6-difluorophenyl)pyrazolyl] to obtain blue/green LECs (λ_{max} = 492 nm) based on complex [Ir(F_2-ppz)$_2$(dtb-bpy)][PF$_6$] [35]. We proposed to use a different N^N ligand with a high-energy LUMO level to develop blue emitters. In this section, the use of the Met$_4$phen N^N ligand (Met$_4$phen is 3,4,7,8-tetramethyl-1,10-phenanthroline), which presents a high-energy LUMO, together with the F_2-ppy C^N ligands, which provide a low-energy HOMO, is presented. The combination of these ligands results in an Ir-iTMC, [Ir(F_2-ppy)$_2$(Met$_4$phen)][PF$_6$] (Fig. 8), with a wide bandgap [42].

The photoluminescence spectrum recorded for [Ir(F_2-ppy)$_2$(Met$_4$phen)][PF$_6$] in de-aerated acetonitrile solution shows a structured band with one intense maximum at 476 nm, a second less intense maximum at 508 nm, and a low-intensity shoulder around 550 nm (Fig. 8). Such a structured emission spectrum indicates a significant contribution from a ligand-centered (LC) π–π* transition. Upon applying an external bias of 3 V to an ITO/PEDOT:PSS/[Ir(F_2-ppy)$_2$(Met$_4$phen)][PF$_6$]/Al LEC device, an increase in the current density and luminance is observed, reaching a low luminance value of 30 cd/m^2 with a maximum power efficiency of 5.8 Lm/W. The color of the emitted light is more striking than the high power efficiency. Instead of the expected blue emission color, the LEC device emits green light (560 nm, CIE coordinates: x = 0.417 and y = 0.533) [82], which implies a shift of 84 nm with respect to the solution-based emission spectrum (Fig. 8).
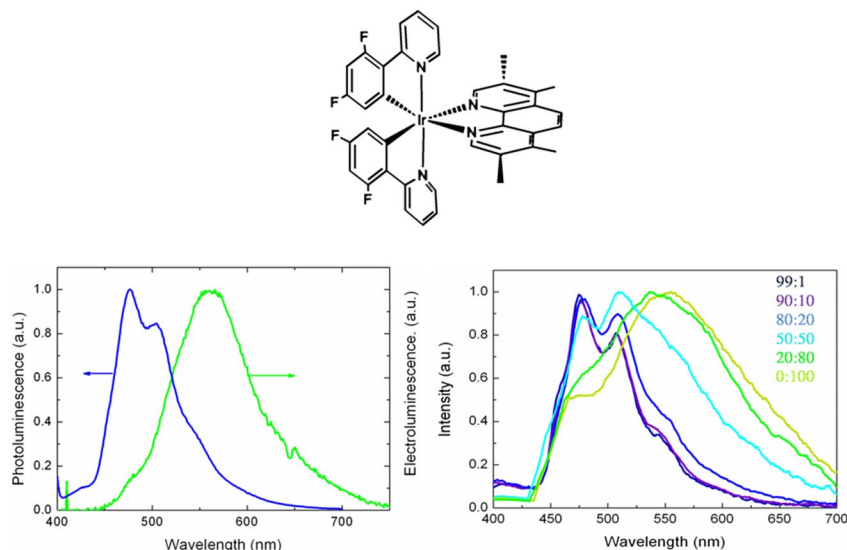
Fig. 8 Top: Chemical structure of the complex [Ir(F$_2$-ppy)$_2$(Met$_4$phen)][PF$_6$]. Bottom: The left graph displays the electroluminescence spectrum of an ITO/PEDOT:PSS/[Ir(F$_2$-ppy)$_2$(Met$_4$phen)][PF$_6$]/Al device (green) and the photoluminescence spectrum of [Ir(F$_2$-ppy)$_2$(Met$_4$phen)][PF$_6$] in acetonitrile solution (blue). The right graph displays the room-temperature emission spectra of thin films of PMMA: [Ir(F$_2$-ppy)$_2$(Met$_4$phen)][PF$_6$] at several molar ratios on quartz substrates (λ_{exc} = 300 nm).

In order to determine the origin of this large red-shift, we studied the photoluminescent properties of a series of thin films of polymethylmethacrylate (PMMA) with increasing amounts of the complex [Ir(F$_2$-ppy)$_2$(Met$_4$phen)][PF$_6$] ranging from 1 to 100 % (Fig. 8). We found that the photoluminescence spectrum of highly diluted films is similar to that obtained from the complex in acetonitrile solution, while the spectrum from concentrated films is more similar to the emission profile obtained in LECs. The observed shift of the emission spectrum for [Ir(F$_2$-ppy)$_2$(Met$_4$phen)][PF$_6$] in an LEC device is primarily related to the concentration and, hence, to the intersite distance of the complex in the solid film. We also discarded the relation between the concentration-dependent emission spectrum and the formation of dimers and/or excimers, which are known to cause a red-shift in the emission spectrum [88]. The commonly observed feature for excimer emission in this type of complex is the increase of the excited-state lifetime. The emission lifetime was studied, showing that it ranges from a few microseconds in a polymer film containing 5 % of the iTMC to a few nanoseconds in the case of the 80 and 100 % doped polymer films. This decrease of the excited-state lifetime ruled out the possibility of excimer emission.

Hence, we proposed another explanation for the observed shift of the emission wavelength. This is related to the different emissive triplet states predicted from quantum chemical calculations. According to these calculations, at least three low-energy triplet states, lying within 0.10 eV, are present in this iTMC. Although the energy difference is small, the estimated vertical emission energies associated with these triplets differ by as much as 60 nm. Hence, the concentration-dependent emission seems to be related to the presence of multiple excited triplet states, whose energetic ordering changes as a function of the local environment of the complex.

Other groups have successfully proposed other ancillary ligands to obtain blue emission in LECs [47,63,64].

CONCLUSION

This short review describes in detail some of the different strategies used to design Ir-iTMCs with the aim to enhance the performances of LECs. They can be summarized as follows: (a) red LECs combining fluorescent emitters and Ir-iTMCs, (b) the use of bulky groups and spacers to reach high efficiencies, (c) stable LECs using π-interactions and blocking groups, and (d) blue LECs using new N^N ligands with high-energy LUMO level. The results obtained to date clearly confirm that LECs are a promising technology for lighting applications. Nonetheless, these findings have been achieved using different iTMCs in LECs. Hence, the main target for the future is to join all these strategies in only one iTMC.

ACKNOWLEDGMENTS

REFERENCES

1. Q. Pei, G. Yu, C. Zhang, Y. Yang, A. J. Heeger. *Science* **269**, 1086 (1995).
2. J. D. Slinker, J. Rivnay, J. S. Moskowitz, J. B. Parker, S. Bernhard, H. D. Abruña, G. G. Malliaras. *J. Mater. Chem.* **17**, 2976 (2007).
3. Q. B. Pei, Y. Yang, G. Yu, C. Zhang, A. J. Heeger. *J. Am. Chem. Soc.* **118**, 3922 (1996).
4. D. J. Dick, A. J. Heeger, Y. Yang, Q. B. Pei. *Adv. Mater.* **8**, 985 (1996).
5. L. Edman. *Electrochim. Acta* **50**, 3878 (2005).
6. P. Matyba, K. Maturova, M. Kemerink, N. D. Robinson, L. Edman. *Nat. Mater.* **8**, 672 (2009).
7. Q. Pei, A. J. Heeger. *Nat. Mater.* **7**, 167 (2008).
8. N. D. Robinson, J. H. Shin, M. Berggren, L. Edman. *Phys. Rev. Lett. B* **74**, 155210 (2006).
9. J. C. deMello. *Phys. Rev. B* **66**, 235210 (2002).
10. J. C. deMello. *Nat. Mater.* **6**, 796 (2007).
11. J. C. deMello, N. Tessler, S. C. Graham, R. H. Friend. *Phys. Rev. B* **57**, 12951 (1998).
12. G. G. Malliaras, J. D. Slinker, J. A. DeFranco, M. J. Jaquith, W. R. Silveira, Y.-W. Zhong, J. M. Moran-Mirabal, H. G. Craighead, H. D. Abruña, J. A. Marohn. *Nat. Mater.* **7**, 168 (2008).
13. J. D. Slinker, J. A. DeFranco, M. J. Jaquith, W. R. Silveira, Y. Zhong, J. M. Moran-Mirabal, H. G. Graighead, H. D. Abruña, J. A. Marohn, G. G. Malliaras. *Nat. Mater.* **6**, 894 (2007).
14. M. Lenes, G. Garcia-Belmonte, D. Tordera, A. Pertegás, J. Bisquert, H. J. Bolink. *Adv. Funct. Mater.* **21**, 1581 (2011).
15. S. van Reenen, P. Matyba, A. Dzwilewski, R. A. J. Janssen, L. Edman, M. Kemerink. *J. Am. Chem. Soc.* **132**, 13776 (2010).
16. F. G. Gao, A. J. Bard. *J. Am. Chem. Soc.* **122**, 7426 (2000).
17. M. Buda, G. Kalyuzhny, A. J. Bard. *J. Am. Chem. Soc.* **124**, 6090 (2002).
18. H. Rudmann, S. Shimada, M. F. Rubner. *J. Am. Chem. Soc.* **124**, 4918 (2002).
19. A. P. Wu, J. K. Lee, M. F. Rubner. *Thin Solid Films* **327–329**, 663 (1998).
20. A. P. Wu, D. S. Yoo, J. K. Lee, M. F. Rubner. *J. Am. Chem. Soc.* **121**, 4883 (1999).

21. K. M. Maness, R. H. Terrill, T. J. Meyer, R. W. Murray, R. M. Wightman. *J. Am. Chem. Soc.* **118**, 10609 (1996).
22. S. Bernhard, X. Gao, G. G. Malliaras, H. D. Abruña. *Adv. Mater.* **14**, 433 (2002).
23. N. Armaroli, G. Accorsi, M. Holler, O. Moudam, J. F. Nierengarten, Z. Zhou, R. T. Wegh, R. Welter. *Adv. Mater.* **18**, 1313 (2006).
24. A. R. Hosseini, C. Y. Koh, J. D. Slinker, S. Flores-Torres, H. D. Abruña, G. G. Malliaras. *Chem. Mater.* **17**, 6114 (2005).
25. Q. Zhang, Q. Zhou, Y. Cheng, L. Wang, D. Ma, X. Jing, F. Wang. *Adv. Funct. Mater.* **16**, 1203 (2006).
26. Y.-M. Wang, F. Teng, Y.-B. Hou, Z. Xu, Y.-S. Wang, W.-F. Fu. *Appl. Phys. Lett.* **87**, 233512 (2005).
27. O. Moudam, A. Kaeser, B. Delavaux-Nicot, C. Duhayon, M. Holler, G. Accorsi, N. Armaroli, I. Séguy, J. Navarro, P. Destruel, J.-F. Nierengarten. *Chem. Commun.* 3077 (2007).
28. F. G. Gao, A. J. Bard. *Chem. Mater.* **14**, 3465 (2002).
29. R. D. Costa, D. Tordera, E. Ortí, H. J. Bolink, J. Schönle, S. Graber, C. E. Housecroft, E. C. Constable, J. A. Zampese. *J. Mater. Chem.* **21**, 16108 (2011).
30. J. D. Slinker, A. A. Gorodetsky, M. S. Lowry, J. Wang, S. Parker, R. Rohl, S. Bernhard, G. G. Malliaras. *J. Am. Chem. Soc.* **126**, 2763 (2004).
31. R. D. Costa, E. Ortí, H. J. Bolink, S. Graber, S. Schaffner, M. Neuburger, C. E. Housecroft, E. C. Constable. *Adv. Funct. Mater.* **19**, 3456 (2009).
32. M. S. Lowry, J. I. Goldsmith, J. D. Slinker, R. Rohl, R. A. Pascal, G. G. Malliaras, S. Bernhard. *Chem. Mater.* **17**, 5712 (2005).
33. S. T. Parker, J. Slinker, M. S. Lowry, M. P. Cox, S. Bernhard, G. G. Malliaras. *Chem. Mater.* **17**, 3187 (2005).
34. J. D. Slinker, C. Y. Koh, G. G. Malliaras, M. S. Lowry, S. Bernhard. *Appl. Phys. Lett.* **86**, 173506 (2005).
35. A. B. Tamayo, S. Garon, T. Sajoto, P. I. Djurovich, I. M. Tsyba, R. Bau, M. E. Thompson. *Inorg. Chem.* **44**, 8723 (2005).
36. H. J. Bolink, L. Cappelli, E. Coronado, M. Graetzel, M. Nazeeruddin. *J. Am. Chem. Soc.* **128**, 46 (2006).
37. H. J. Bolink, L. Cappelli, E. Coronado, M. Graetzel, E. Ortí, R. D. Costa, M. Viruela, M. K. Nazeeruddin. *J. Am. Chem. Soc.* **128**, 14786 (2006).
38. H. J. Bolink, L. Cappelli, E. Coronado, A. Parham, P. Stössel. *Chem. Mater.* **18**, 2778 (2006).
39. M. S. Lowry, S. Bernhard. *Chem.—Eur. J.* **12**, 7970 (2006).
40. M. K. Nazeeruddin, R. T. Wegh, Z. Zhou, C. Klein, Q. Wang, F. De Angelis, S. Fantacci, M. Graetzel. *Inorg. Chem.* **45**, 9245 (2006).
41. H. C. Su, C. C. Wu, F. C. Fang, K. T. Wong. *Appl. Phys. Lett.* **89**, 261118 (2006).
42. H. J. Bolink, L. Cappelli, S. Cheylan, E. Coronado, R. D. Costa, N. Lardies, M. K. Nazeeruddin, E. Ortí. *J. Mater. Chem.* **17**, 5032 (2007).
43. H. C. Su, F. C. Fang, T. Y. Hwu, H. H. Hsieh, H. Chen, G. Lee, S. Peng, K. T. Wong, C. C. Wu. *Adv. Funct. Mater.* **17**, 1019 (2007).
44. H. J. Bolink, E. Coronado, R. D. Costa, N. Lardiés, E. Ortí. *Inorg. Chem.* **47**, 9149 (2008).
45. H. J. Bolink, E. Coronado, R. D. Costa, E. Ortí, M. Sessolo, S. Graber, K. Doyle, M. Neuburger, C. E. Housecroft, E. C. Constable. *Adv. Mater.* **20**, 3910 (2008).
46. S. Graber, K. Doyle, M. Neuburger, C. E. Housecroft, E. C. Constable, R. D. Costa, E. Ortí, D. Repetto, H. J. Bolink. *J. Am. Chem. Soc.* **130**, 14944 (2008).
47. L. He, L. Duan, J. Qiao, R. Wang, P. Wei, L. Wang, Y. Qiu. *Adv. Funct. Mater.* **18**, 2123 (2008).
48. H. C. Su, H. F. Chen, F. C. Fang, C. C. Liu, C. C. Wu, K. T. Wong, Y. H. Liu, S. M. Peng. *J. Am. Chem. Soc.* **130**, 3413 (2008).
49. H.-C. Su, H.-F. Chen, C.-C. Wu, K.-T. Wong. *Chem. Asian J.* **3**, 1922 (2008).

50. E. Zysman-Colman, J. D. Slinker, J. B. Parker, G. G. Malliaras, S. Bernhard. *Chem. Mater.* **20**, 388 (2008).

51. R. D. Costa, F. J. Céspedes-Guirao, E. Ortí, H. J. Bolink, J. Gierschner, F. Fernández-Lázaro, A. Sastre-Santos. *Chem. Commun.* 3886 (2009).

52. R. D. Costa, E. Ortí, H. J. Bolink, S. Graber, C. E. Housecroft, M. Neuburger, S. Schaffner, E. C. Constable. *Chem. Commun.* 2029 (2009).

53. L. He, J. Qiao, L. Duan, G. Dong, D. Zhang, L. Wang, Y. Qiu. *Adv. Funct. Mater.* **19**, 2950 (2009).

54. T.-H. Kwon, Y. H. Oh, I.-S. Shin, J.-I. Hong. *Adv. Funct. Mater.* **19**, 711 (2009).

55. E. Margapoti, V. Shukla, A. Valore, A. Sharma, C. Dragonetti, C. C. Kitts, D. Roberto, M. Murgia, R. Ugo, M. Muccini. *J. Phys. Chem. C* **113**, 12517 (2009).

56. J. L. Rodríguez-Redondo, R. D. Costa, E. Ortí, A. Sastre-Santos, H. J. Bolink, F. Fernández-Lázaro. *Dalton Trans.* 9787 (2009).

57. C. Rothe, C.-J. Chiang, V. Jankus, K. Abdullah, X. Zeng, R. Jitchati, A. S. Batsanov, M. R. Bryce, A. P. Monkman. *Adv. Funct. Mater.* **19**, 2038 (2009).

58. R. D. Costa, G. Fernandez, L. Sanchez, N. Martin, E. Ortí, H. J. Bolink. *Chem.–Eur. J.* **16**, 9855 (2010).

59. R. D. Costa, E. Ortí, H. J. Bolink, S. Graber, C. E. Housecroft, E. C. Constable. *Adv. Funct. Mater.* **20**, 1511 (2010).

60. R. D. Costa, E. Ortí, H. J. Bolink, S. Graber, C. E. Housecroft, E. C. Constable. *J. Am. Chem. Soc.* **132**, 5978 (2010).

61. R. D. Costa, A. Pertegás, E. Ortí, H. J. Bolink. *Chem. Mater.* **22**, 1288 (2010).

62. L. He, L. Duan, J. Qiao, G. Dong, L. Wang, Y. Qi. *Chem. Mater.* **22**, 3535 (2010).

63. M. Mydlak, C. Bizzarri, D. Hartmann, W. Sarfert, G. Schmid, L. De Cola. *Adv. Funct. Mater.* **20**, 1812 (2010).

64. C.-H. Yang, J. Beltran, V. Lemaur, J. Cornil, D. Hartmann, W. Sarfert, R. Frohlich, C. Bizzarri, L. De Cola. *Inorg. Chem.* **49**, 9891 (2010).

65. R. D. Costa, E. Ortí, H. J. Bolink, S. Graber, C. E. Housecroft, E. C. Constable. *Chem. Commun.* **47**, 3207 (2011).

66. R. D. Costa, E. Ortí, D. Tordera, A. Pertegás, H. J. Bolink, S. Graber, C. E. Housecroft, L. Sachno, M. Neuburger, E. C. Constable. *Adv. Energy Mater.* **1**, 282 (2011).

67. L. He, L. Duan, J. Qiao, D. Zhang, L. Wang, Y. Qiu. *Chem. Commun.* **47**, 6467 (2011).

68. F. Alary, J. L. Heully, L. Bijeire, P. Vicendo. *Inorg. Chem.* **46**, 3154 (2007).

69. V. Balzani, S. Campagna (Eds.). *Photochemistry and Photophysics of Coordination Compounds I and II*, Vol. 280, Springer (2007).

70. B. Durham, J. V. Caspar, J. K. Nagle, T. J. Meyer. *J. Am. Chem. Soc.* **104**, 4803 (1982).

71. D. W. Thompson, J. F. Wishart, B. S. Brunschwig, N. Sutin. *J. Phys. Chem. A* **105**, 8117 (2001).

72. J. Van Houten, R. J. Watts. *J. Am. Chem. Soc.* **98**, 4853 (1976).

73. H. Yersin. *Triplet Emitters for OLED Applications. Mechanism of Exciton Trapping and Control of Emission Properties*, Springer (2004).

74. M. S. Lowry, W. R. Hudson, R. A. Pascal, S. Bernhard. *J. Am. Chem. Soc.* **126**, 14129 (2004).

75. F. Neve, A. Crispini, S. Campagna, S. Serroni. *Inorg. Chem.* **38**, 2250 (1999).

76. C. Ulbricht, B. Beyer, C. Friebe, A. Winter, U. S. Schubert. *Adv. Mater.* **21**, 4418 (2009).

77. H. J. Bolink, L. Cappelli, E. Coronado, P. Gaviña. *Inorg. Chem.* **44**, 5966 (2005).

78. H. J. Bolink, E. Coronado, R. D. Costa, E. Ortí, P. Gaviña, S. Tatay. *Inorg. Chem.* **48**, 3907 (2009).

79. R. D. Costa, F. J. Céspedes-Guirao, H. J. Bolink, F. Fernández-Lázaro, A. Sastre-Santos, E. Ortí, J. Gierschner. *J. Phys. Chem. C* **113**, 19292 (2009).

80. F. Würthner. *Chem. Commun.* 1564 (2004).

81. R. Gvishi, R. Reisfeld, Z. Burshtein. *Chem. Phys. Lett.* 213 (1993).

82. CIE 1933.

83. D. R. Blasini, J. Rivnay, D. M. Smilgies, J. D. Slinker, S. Flores-Torres, H. D. Abruña, G. G. Malliaras. *J. Mater. Chem.* **17**, 1458 (2007).
84. G. Kalyuzhny, M. Buda, J. McNeill, P. Barbara, A. J. Bard. *J. Am. Chem. Soc.* **125**, 6272 (2003).
85. L. J. Soltzberg, J. Slinker, S. Flores-Torres, D. Bernards, G. G. Malliaras, H. D. Abruna, J. S. Kim, R. H. Friend, M. D. Kaplan, V. Goldberg. *J. Am. Chem. Soc.* **128**, 7761 (2006).
86. J. D. Slinker, J.-S. Kim, S. Flores-Torres, J. H. Delcamp, H. D. Abruña, R. H. Friend, G. G. Malliaras. *J. Mater. Chem.* **7**, 76 (2007).
87. S. Bernhard, J. A. Barron, P. L. Houston, H. D. Abruna, J. L. Ruglovksy, X. C. Gao, G. G. Malliaras. *J. Am. Chem. Soc.* **124**, 13624 (2002).
88. J. B. Birks. *Rep. Prog. Phys.* **38**, 903 (1975).